Predicting the ultimate potential of natural gas SOFC power cycles with CO_2 capture – Part B: Applications

Stefano Campanari [a, *, 1], Luca Mastropasqua [a, 1], Matteo Gazzani [b], Paolo Chiesa [a, 1], Matteo C. Romano [a, 1]

[a] *Politecnico di Milano, Department of Energy, Via Lambruschini 4, 20156 Milano, Italy*
[b] *ETHZ, Institute of Process Engineering, Sonneggstrasse 3, 8092 Zurich, Switzerland*

An important advantage of solid oxide fuel cells (SOFC) as future systems for large scale power gener-ation is the possibility of being efficiently integrated with processes for CO_2 capture. Focusing on natural gas power generation, Part A of this work assessed the performances of advanced pressurised and atmospheric plant configurations (SOFC + GT and SOFC + ST, with fuel cell integration within a gas turbine or a steam turbine cycle) without CO_2 separation. This Part B paper investigates such kind of power cycles when applied to CO_2 capture, proposing two ultra-high efficiency plant configurations based on advanced intermediate-temperature SOFCs with internal reforming and low temperature CO_2 separation process. The power plants are simulated at the 100 MW scale with a set of realistic assumptions about FC performances, main components and auxiliaries, and show the capability of exceeding 70% LHV efficiency with high CO_2 capture (above 80%) and a low specific primary energy consumption for the CO_2 avoided (1.1–2.4 MJ kg^{-1}). Detailed results are presented in terms of energy and material balances, and a sensitivity analysis of plant performance is developed vs. FC voltage and fuel utilisation to investigate possible long-term improvements. Options for further improvement of the CO_2 capture efficiency are also addressed.

Keywords:
SOFC power cycle
Hybrid cycle
Natural gas
CO2 capture

1. Introduction

Given current concerns about global warming, Carbon Capture and Sequestration can play a key role in limiting the increase of CO_2 concentration in the atmosphere [1]. Although different commercial technologies can be applied to perform CO_2 capture, all of them entail a conversion efficiency decay along with an increase of the plant investment. For instance, flue gas decarbonisation via chemical absorption-stripper processes (e.g. with amines in a so-called 'post-combustion' arrangement), often regarded as one of the most viable technologies, brings about high energy requirements and net efficiency penalties [2,3] and the same applies to oxy-combustion and fuel decarbonisation processes [4]. Indeed, several promising technologies are currently being developed both at lab and pilot scale to partially overcome these drawbacks [5,6]. Within this framework, fuel cells (FC) share the unique capability of bridging high efficiency with the possibility of capturing the produced CO_2. Alongside the investigation of long-term solutions, as direct or indirect coal-based fuel cells [7–9], part of current

* Corresponding author.
E-mail address: stefano.campanari@polimi.it (S. Campanari).
[1] www.gecos.polimi.it.

Published Journal Article available at: http://dx.doi.org/10.1016/j.jpowsour.2016.05.134

Nomenclature

FC	fuel cell
GT	gas turbine
HHV	higher heating value, [MJ kg^{-1}]
HT	high temperature
HTS	high temperature shift
HRSG	heat recovery steam generator
LHV	lower heating value, [MJ kg^{-1}]
LT	low temperature
m	mass flow rate, [kg s^{-1}]
NG	natural gas
ORC	organic Rankine cycle
P	power, [MW]
p	total pressure, [bar]
Q	mole flow rate, [kg s^{-1}]
S	entropy, [kW K^{-1}]
SOFC	solid oxide fuel cell
ST	steam turbine
T	temperature, [°C or K]
U_a	air utilisation factor: $U_a = O_{2,consumed}/O_{2,inlet}$
U_f	Fuel utilisation factor
V	fuel cell potential, [V]
WGS	water gas shift

Subscripts

a	air
amb	ambient
el	electric
in	inlet
f	fuel
th	thermal

research on power production from fuel cells with CO_2 capture is focused on the use of natural gas (NG) as fuel [10–15]. With the aim of maximizing the plant efficiency, high temperature fuel cells are the preferred choice because of the possibility of matching the heat balance of the natural gas conversion route with the fuel cell. Especially, SOFC has demonstrated the potential to reach 60% + LHV electrical efficiency from natural gas even at a few kW scale [16–19]. Besides the intrinsic efficiency gain induced by the SOFC electrochemical oxidation, the depleted fuel and the exhaust gases are not mixed with nitrogen, which makes the gas compo-sition particularly suitable for an efficient CO_2 removal process. Additionally, one of the SOFC key advantages is the possibility to sustain internally the natural gas reforming process, exploiting the fuel cell exhaust heat to drive the endothermic reforming reactions. Depending on the SOFC integration with the natural gas reforming and shift section, two main configurations can be identified: (i) systems where natural gas is internally reformed in the FC, and (ii) systems where natural gas is reformed upstream the FC, which is therefore fed with mainly hydrogen. As shown in a previous paper [20] and thoroughly discussed in Part A of this paper, the second option leads to lower performance and to a very demanding heat exchange network. Therefore, only configurations with internal FC reforming of natural gas have been considered in this work.

The goal of this paper is to provide an overall picture of the ultimate performance of NG-fuelled, SOFC-based, power cycles with CO_2 capture by predicting and comparing the results on the grounds of consistent assumptions and common methodology. Following Part A, where the methodology, the SOFC technology level and the reference cases without CO_2 capture are discussed, this Part B paper discusses their application to CO_2 capture, integrating the separation process into SOFC cycles. Firstly, the CO_2 separation technology adopted in this work (cryogenic CO_2 condensation) is described. Afterwards, two different hybrid cycles with CO_2 capture derived from the reference cases discussed in Part A are presented: (i) ambient pressure SOFC coupled with steam-based, Rankine cycle, and (ii) pressurised SOFC coupled with a Brayton cycle. The analysis is completed with additional sensitivity analyses on the main operating variables.

2. Analysis of the power plants with CO_2 capture

The analysis is developed with the same modelling tools introduced in Part A of the work, e.g. the in-house code GS for the power plant [21–23] with the addition of ASPEN Plus™ for the simulation of the CO_2 cryogenic and compression sections [24]. Both the plant configurations presented here are based on the reference layout discussed in Part A of the work: the design point is kept constant for all components but for those requiring modifications to apply CO_2 capture. In particular, simulations are carried out with the same overall assumptions discussed in part A of the work, with the addition of case-specific hypotheses (discussed hereafter) and other miscellaneous calculation constraints listed in Table 1.

As far as the SOFC is concerned, the cell voltage and the attained fuel utilisation factor are varied with a sensitivity analysis to characterise their effects on the overall balance of plant when CCS is applied. The cell modular configuration is assumed to reproduce on a larger scale the state-of-the-art SOFC performances discussed in Part A, featuring a 60% + net electric efficiency.

In the considered plant configurations, provided that the CO_2 concentration of the stream at the SOFC anode outlet is about 60% (dry basis), cryogenic systems embody a promising option to separate the CO_2 from the remaining gases included in the mixture. However, independently of the type of power cycle considered, the anode exhaust stream exiting the SOFC requires an additional purification process to recover the heating value of the unconverted fuel species (at the 85% fuel utilisation stipulated in the work, around 2 MJ kg^{-1}_{LHV}) and achieve the required CO_2 purity (i.e. >96% [25]). In particular, subsequently to anode off-gas heat recovery, necessary for the gas or steam cycle integration, a single high temperature water-gas-shift reactor is envisaged (we avoid considering more complex schemes with two reactors at different temperatures), which performs the conversion of residual carbon monoxide to CO_2, according to the reaction:

$$CO + H_2O \leftrightarrow CO_2 + H_2 \quad \Delta H^{\circ}_r = -41.1 \text{ kJ mol}^{-1} \qquad (1)$$

The resulting stream is then sent to a CO_2 removal section based

Table 1
Additional simulation assumptions for the power cycles with CCS (see part A of the work for all other assumptions).

HT WGS reactor	
HT WGS inlet temperature [°C]	340.0
HT WGS pressure drop [%]	2.0%
Heat transfer loop (SOFC + GT cycle with CO_2 capture)	
CO_2 blower isentropic/mechanical efficiency [%]	0.88/0.94
Operating pressure of CO_2 loop [bar]	20.0
Maximum operating temperature CO_2 blower [°C]	480.0

on a cryogenic process. Residual fuel compounds (mainly containing hydrogen) are recycled to the power plant. Finally, high purity CO_2 stream obtained at the end of the process is taken to supercritical pressure for storage [26].

The anode stream has therefore to be cooled to a temperature approaching the triple point of CO_2 (−56.6 °C), so that most of the CO_2 condenses and can be separated by gravity from the fuel species which have much lower boiling point and therefore mostly remain in the gaseous phase.

Two configurations can be adopted to cool down the stream to be purified:

1) a self-refrigerated system where the CO_2 separated in the circuit is the working fluid of the refrigerating cycle required to cool the mixture [27];
2) an external multi evaporation level compression chiller. Since heat has to be removed at temperature below the CO2 triple point, with a significantly large temperature difference with respect to the ambient temperature, binary refrigerating loops (e.g. propane/ethane or propane/ethylene loops) are generally proposed.

Preliminary techno-economic analyses [28] show that the first solution offers simpler equipment and plant layout, and lower investment and operating costs than the external chillers. Performance assessment in this paper is therefore based on a self-refrigerated system whose flowsheet, similar to the one proposed in Ref. [29], is shown in Fig. 1.

Firstly, the CO_2-rich stream from the cell anode is compressed at 40 bar in an intercooled compression train where water is progressively removed by condensation. To prevent ice formation in the following cold section, the gas is dehydrated by means of molecular sieves.

The pressurised and dehydrated stream is then cooled and partially condensed in the multi-flow heat exchanger, HE1. The following knockout drum 1 separates the liquid condensed at −33 °C in order to reduce the flow rate to the low temperature section and to decrease the overall compression load. The liquid separated in the knockout drum 1 is throttled through the valve TV1 that brings about the temperature drop necessary to keep a 3 °C minimum approach inside HE1. To enhance the separation factor, the vapour fraction exiting the knockout drum 1 is further cooled down to −53 °C in the exchanger HE2. At this temperature more CO_2 is condensed and separated in the knockout drum 2. An expansion train recovers energy from the non-condensable gas fraction: the vapour fraction exiting the second knockout drum is recycled back to HE2 and then to HE1 to recover part of its thermal content and expanded in a series of three expanders in order to recover its pressure-related energy. The separation pressure (hereby selected at 40 bar) embodies an optimization parameter, which results from a techno-economic and environmental trade-off between the CO_2 removal efficiency and the purity of the liquefied stream; in addition, it affects the dry ice formation issue, especially at the outlet of the throttling valves and at the outlet of the expanders. The CO_2-rich stream separated in the drums (liquid fraction) is then throttled to provide chilling power for impure CO_2 cooling and compressed in an intercooled compression train up to 89.1 bar and finally pumped in liquid phase to 150 bar for long-range transportation and storage. According to calculation carried out, the process attains a CO_2 recovery efficiency of 85.6% and a CO_2 stream purity of 98.8% (mol basis). The vapour fraction exiting drum 2 is then burned with the SOFC cathode off-gas, before feeding the steam cycle or the gas turbine. All assumptions required

Table 2
Assumptions for the CO_2 separation unit in SOFC-based power plant with CCS (other assumptions according to Part A of the work).

Low temperature CO_2 separation unit (double flash)	
Equation of state	Peng-Robinson [30]
LT flash temperature [°C]	−53.0
HT flash temperature [°C]	−33.0
Maximum separation pressure [bar]	40
Minimum ΔT in the heat exchangers [°C]	3
LP/HP compressors inter-coolers number [−]	3/2
Isentropic/mechanical/electric efficiency [%]	82.0/94.0/96.0
Inter-coolers outlet temperature [°C]	30
Inter-coolers pressure losses [%]	1% of inlet pressure
Liquid CO_2 conditions at pump inlet	23 °C, 89.1 bar
Liquid CO_2 to storage	150 bar

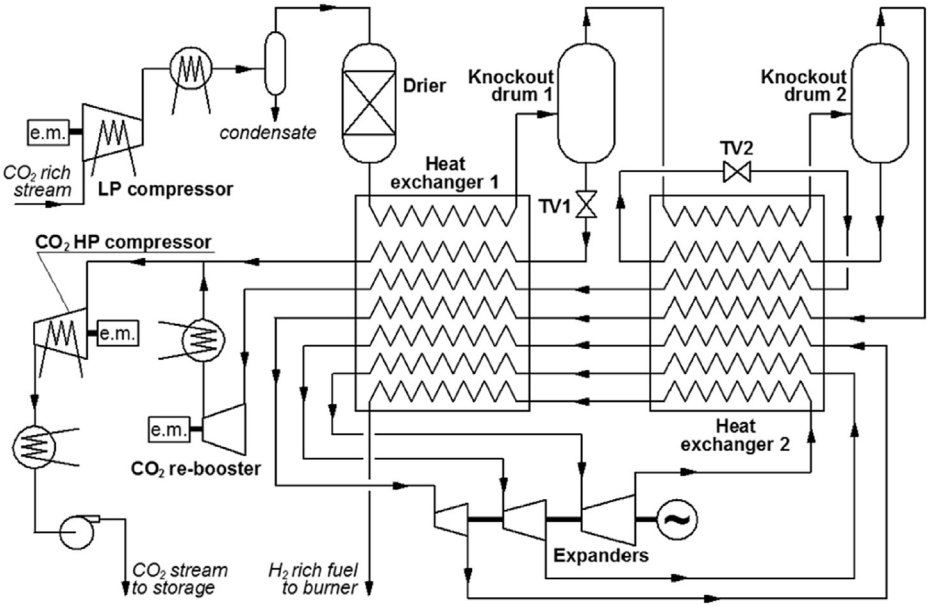

Fig. 1. Layout of the low temperature CO2 separation and compression section (HE = heat exchanger; TV = throttling valve; HP/LP = high/low pressure).

to calculate the cryogenic purification section are listed in Table 2.

3. Atmospheric pressure SOFC + ST cycle with cryogenic CO_2 capture

Fig. 2 shows the power plant configuration for the atmospheric case with CCS. It can be noticed that the configuration of the fuel pre-treating and the SOFC sections is not affected by the CO_2 capture, thus resulting similar to the cases without capture presented in Part A. After fuel desulphurisation, pressurised NG is fed to the SOFC module throughout an ejector, which supplies water to the reforming reaction by recycling the anodic products. A pre-reforming reactor cracks the heavier hydrocarbons contained in the fuel in order to limit the risk of carbon deposition and the heat duty of direct internal reforming reactions occurring within the fuel cell, enhancing in this way the lifetime expectations of the stack itself. The SOFC stack is operated at approximately 1.2 bar, neces-sary to overcome the pressure losses on both air and fuel piping system. Ejector recycling, widely considered for SOFC applications [31], is easily sustained by grid NG pressure, assumed at 20 bar.

Differently from the case without CO_2 capture, the energy content of the anodic spent fuel and the cathode exhaust is recovered without direct mixing. In this instance, the single level steam cycle is subdivided using two different steam generators: (i) the first produces superheated steam at 400 °C and 40 bar from the anodic stream (downstream the recycle branching), which is cooled from 800 °C to the required inlet temperature for the WGS reactor (340 °C); (ii) the second produces steam of the same quality (400 °C, 40 bar) from the cathode exhaust line, downstream the residual fuel combustor. The overall amount of steam produced is expanded in the same steam turbine. Fig. 3 reports the temperature – heat duty-diagram of the two exhaust gas heat exchange processes with the steam cycle working fluid.

After recovering most of the available thermal power in the anode exhaust, a high temperature water gas shift (HT-WGS) reactor is used to convert most of the carbon monoxide into hydrogen and CO_2, thus increasing the amount of carbon dioxide in the spent fuel and the CO_2 recovery of the plant. In order to limit the plant costs and to reduce the amount of catalyst required, no LT-WGS reactor is adopted.

The simulation of the WGS reactor is carried out at equilibrium, which may imply minor deviations in the outlet composition and temperature; the reactor is considered to work with typical high temperature chromium iron-promoted catalysts supported on an alumina mesh. The reactor volume and design, which are very important for an economic analysis, are not assessed in this work. The attained CO conversion is about 83% at the chosen operating conditions, thus entailing that approximately 2.9% of the total carbon atoms are still present as carbon monoxide at the WGS reactor outlet. As shown in Fig. 3, the exothermic WGS reaction leads to a temperature rise of about 49 °C. Subsequently to heat recovery and cooling down to nearly ambient temperature, CO_2 is separated in the cryogenic process previously described. The H_2-rich fuel gas recovered is preheated and burned with the SOFC cathode exhaust gas. The total pressure drop in the anode exhaust line (from #17 to #27) is approximately 0.2 bar, of which ~0.14 bar from the WGS reactor inlet to the cryogenic section inlet, which is evaluated a reasonable figure; pressure drops are here for simplicity equally split (2% across each component in the loop from #21 to #27).

It is worth noting that the use of a steam power cycle allows recovering the thermal power available from the FC system within a

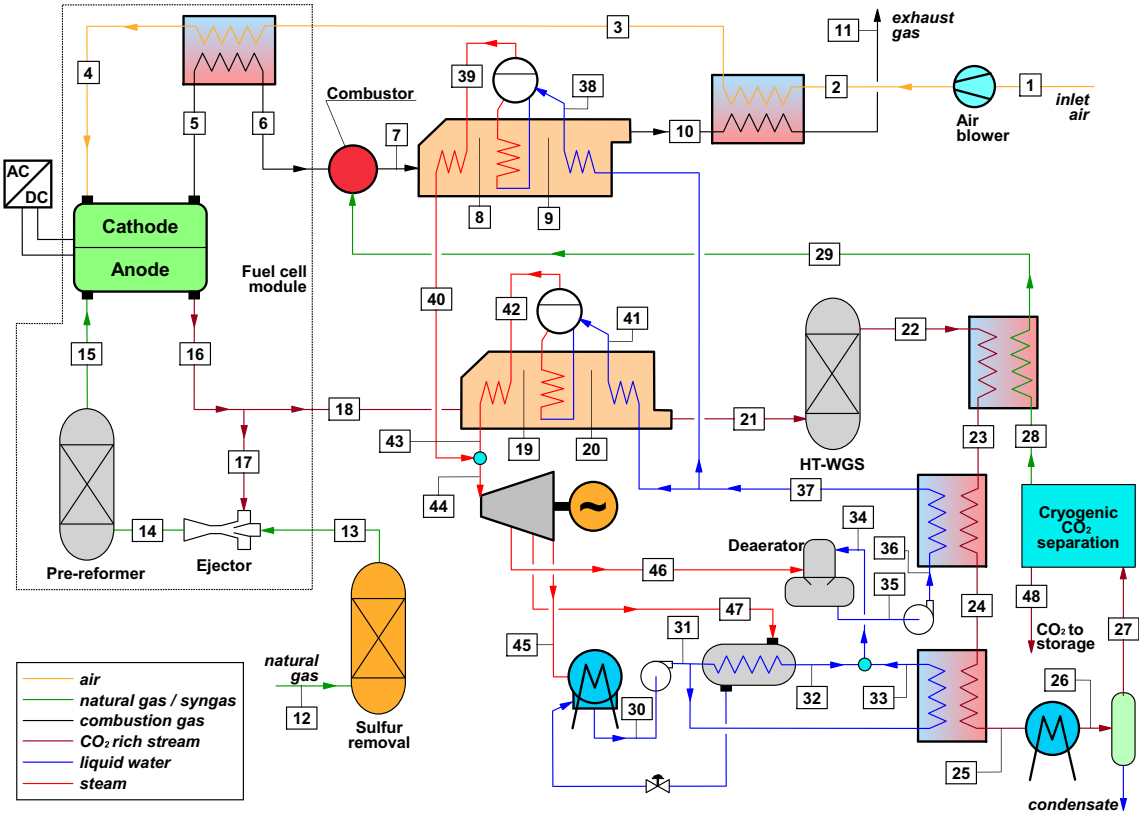

Fig. 2. Atmospheric SOFC-based power plant (SOFC + ST) with CO_2 capture section. The CO_2 separation and compression island has been sketched in a simplified way in order to show the interconnections with the plant components. For a detailed representation of the cryogenic process, the reader may refer to Fig. 1.

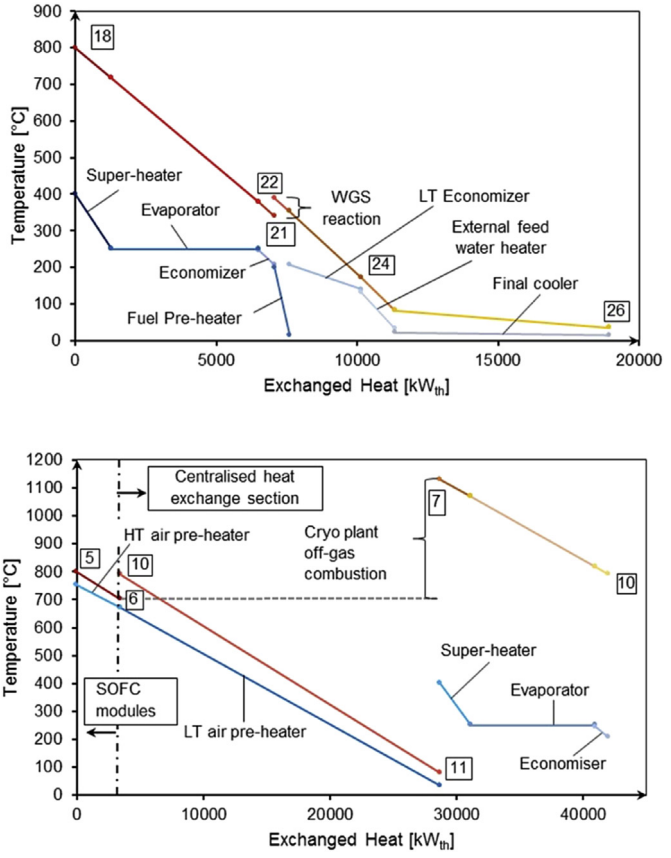

Fig. 3. Cumulative Temperature-Heat duty diagram of anode spent fuel (stream #18 in Fig. 2) cooling section (above) and of cathode exhaust gases (stream #5 in Fig. 2) cooling section (below).

wide range of temperatures. Waste heat dissipations are therefore minimized and limited to very low temperature heat, while most of the valuable heat is recovered by the steam cycle heat exchangers. As it can be seen in Fig. 2, two additional heat exchangers are used to recover the low temperature heat, namely external low temperature economiser and an external feed water heater. These heat exchangers allow enhancing the waste heat recovery from the anode exhaust, reducing the steam flow rate to be bled from the steam turbine for regenerative feed water preheaters. As far as the air heating section is concerned, the cathodic air is heated up using two heat exchangers, similarly to the reference case without CCS. The high temperature HE exploits the heat in the depleted air of the fuel cell at 800 °C, while the low temperature HE makes use of the remaining thermal power in the exhaust gases. The air pre-heating section heat exchange diagram is reported in Fig. 4. The characteristics of the streams of this configuration are reported in Table 3. The thermodynamic conditions and the configuration of the steam plant are consistent with those reported in Consonni et al.[32] for a waste-to-energy application, featuring a very similar medium-scale steam cycle configuration. Based on the correlation between the steam turbine rotational speed and its size suggested by the authors, the steam turbine is operated here at 10000 rpm. Its isentropic efficiency has been set to 85%, reflecting an optimised design [33].

With respect to the corresponding plant without CO_2 capture, the steam bottoming plant operates with larger temperature differences between the combustor exhaust gases and the working fluid ($\Delta T_{min}^{9-38} = 571.24°C$, vs. $\Delta T_{\min}^{9-21} = 15°C = \Delta T_{pp} + \Delta T_{sc}$). The main reason is related to the imposed constraint on the minimum temperature differences on the plant heat exchangers ($\Delta T_{min} = 30°C$), and especially on the HT air pre-heater. In order to respect this limit, which affects the cold end of the HE, it is necessary to reduce the thermal energy subtracted from the cathode outlet stream. In other words, in order to reach the same cathode inlet temperature, the low temperature air pre-heater features a higher thermal duty as compared to the case without CO_2 capture. Ultimately, this is a consequence of the different heat capacity of the gases. In this plant the hot cathode exhaust has a lower heat capacity than the cold air, since its mass flow rate reduces along the SOFC due to oxygen permeation through the electrolyte. As a consequence, the minimum temperature difference in the air preheater is located on the cold end of the heat exchanger. On the contrary, in the plant without capture, hot SOFC exhaust used for air preheating results from combustion between cathode and anode exhaust, so that its flow rate and heat capacity are higher than the cold air.

4. Pressurised SOFC + GT cycle with cryogenic CO_2 capture

The configuration of the pressurised SOFC-based power plant with CO_2 capture is depicted in Fig. 4. Following the desulphurisation treatment, natural gas is heated up to 200 °C in a recuperative heat exchanger. Differently from the discussed atmospheric case, where the fuel preheating would lead to lower steam generation and lower overall power output, a fuel pre-heating is highly beneficial for the pressurised SOFC plant due to the lack of alternatives for low temperature heat recovery in case of the Brayton cycle. The components of the 'SOFC module' highlighted in Fig. 4 work under the same assumptions as those used in the previous case but for the pressure, which is increased to comply with the gas turbine engine. Considering the performance of the SOFC stack, the assumption of keeping the cell voltage constant leads to results in line with the atmospheric application. Indeed, this is a conservative approach as, thanks to the positive pressure effect on the reactant concentrations (linked to the ideal cell potential by the Nernst equation, see Eq. (2)), a higher voltage can be achieved when the cell is operated at the same current density, making the SOFC more efficient. Conversely, if the pressurised plant was operated at the same voltage but at higher current densities, smaller cell stacks could be employed allowing to improve the plant compactness (also favoured by the moderate pressure considered here in terms of pipes and vessels volumes).

$$E_{H_2} = E^0_{H_2}(T) + \frac{RT}{2F}\frac{\ln\left(x_{H_2} x_{O_2}^{0.5} p_{cat}^{0.5}\right)}{x_{H_2O}} \quad (2)$$

In order to reach the SOFC cathode inlet temperature of 735 °C, a three step air preheating is adopted: (i) low temperature with a recuperative heat exchanger from the gas turbine exhausts, (ii) intermediate temperature, with indirect heat recovery from the anode exhaust by means of a CO_2 closed loop, and (iii) high temperature, with direct heat exchange of the hot cathode exhaust. While the low and intermediate temperature heat exchangers would most likely be centralized, the last high temperature recovery could be distributed throughout all the SOFC stack modules, thus reducing the temperature of the pipe supplying the cathode exhaust to the centralized gas turbine combustor. Consequently, a cheaper piping system could be designed.

In the process of air preheating by heat recovery of the anode exhaust gas, a safety constraint raises because an oxidant-fuel heat exchanger (with flammability risks in case of leakages) ought to be employed. In order to overcome this issue, a loop of an inert and safe heat transfer fluid (CO_2) is used as a thermal interconnection

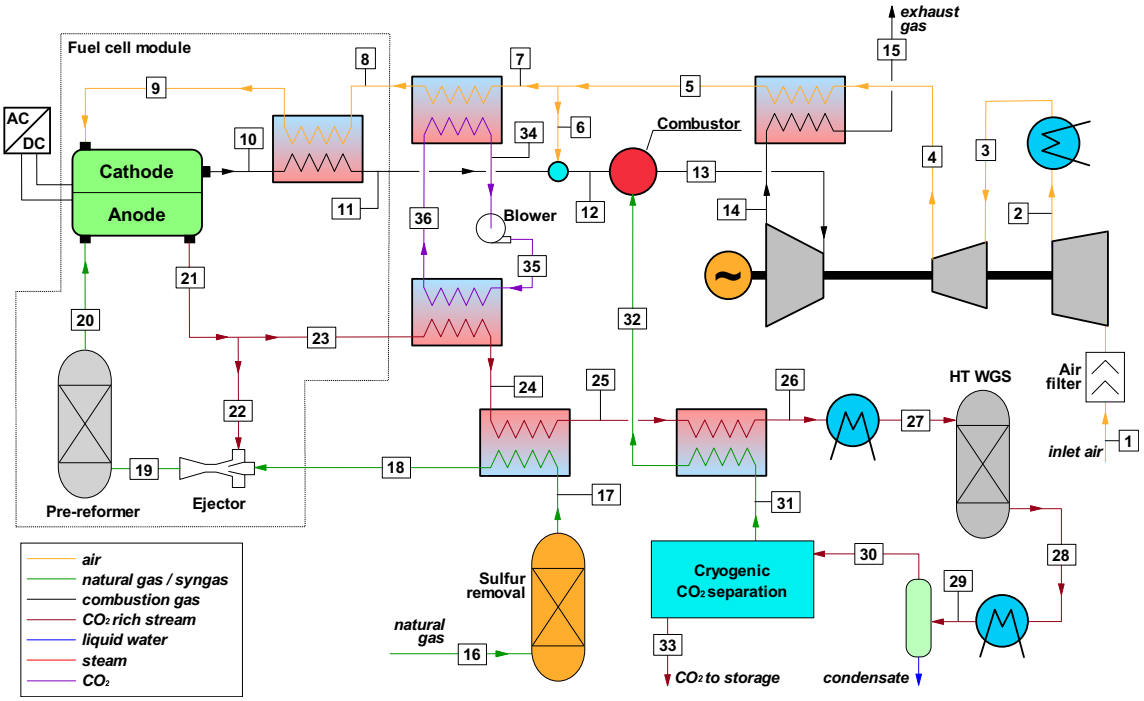

Fig. 4. Pressurised SOFC + GT plant with CO_2 capture section.

between the two streams. The design operating conditions of the CO_2 loop have been selected by a compromise of different technological and thermodynamic considerations. In particular, setting the minimum temperature difference in the HT air/CO_2 heat exchanger at 30 °C and the maximum temperature of the CO_2 at blower inlet (stream #34 in Fig. 4) at 480 °C, the gas turbine recuperative heat exchanger outlet (stream #5) temperature is 450 °C. This temperature T_5 greatly affects the TIT of the gas turbine or the required dilution with fresh air (stream #6) to achieve the target TIT: the higher its value, the higher the air temperature at HT heater inlet (point #8) and the smaller the thermal power required from the cathodic spent air cooling (i.e. the higher the temperature of stream #11). Ultimately, an economic analysis taking into account the cost of heat exchangers and CO_2 blower would be needed to define the optimal T_5 and T_{34}. Both these components are in fact characterised by demanding constraints in terms of maximum operating temperatures; however, examples of components befitting such operating conditions may be found. As far as the former one is concerned, typical high temperature resistant heat exchangers are the diffusion bonded micro-channel heat exchangers usually employed in supercritical CO_2 Brighton cycles [34]. Moreover, the CO_2 high temperature blower operating conditions are less demanding than those already tested by MCFC manufacturers in pressurised plants [35,36].

The non-recycled anodic outlet stream, which is mainly made up of H_2, H_2O and CO_2, as reported in Table 4 (stream #23), is sent to a heat recovery section, whose temperature-heat duty diagram is reported in Fig. 5.

The available thermal power is used, other than to pre-heat air (through the closed CO_2 loop) and natural gas, also to heat up the hydrogen-rich fuel coming from the cryogenic CO_2 condensation section prior to feeding to the GT combustor. Similarly to the atmospheric case, a high temperature WGS reactor is adopted to shift most of the CO content to CO_2. It is worth noting that, as no low temperature heat recovery is used, the sensible energy of the stream leaving the WGS reactor is lost and released to the environment, prior entering the cryogenic CO_2 condensation process. Additionally, to cope with the working temperature range of the WGS reactor, also part of the sensible energy of the inlet stream is wasted to the environment. In total, 13.75% of the plant thermal input is dissipated, of which 1.23 MW above 425 °C and 12.24 MW below 389 °C (see Fig. 5). Recovery of this waste heat is not possible via the gas turbine cycle employed in this case, but in principle could be recovered by adopting a dedicated bottoming thermodynamic cycle, like an ORC (Organic Rankine Cycle). Assuming a reference electric efficiency of around 20% [37] and considering the available thermal energy (13.47 MW), the addition of an ORC cycle would allow gaining 2.6% points in the net electrical efficiency of the overall plant. Overall mass and energy balances of the plant streams are reported in Table 4.

If we compare this cycle layout with the corresponding cycle without CCS, the main modifications introduced are: (i) the anodic spent fuel cooling section (ii) the WGS reactor, and (iii) the cryogenic section. This embodies the reason for the differences in the operating conditions of the overall power plant in the two cases. Concerning the SOFC operation, it is important to underline the different cathode inlet temperature: in this configuration, the cell works with an air inlet temperature $T_a = 735$ °C, whilst in the reference case without CCS, the same SOFC operates at $T_a = 752.2$ °C. In fact, in the former case natural gas pre-heating is performed in order to recover part of the excess heat from anode exhaust cooling, thus increasing the advancement of reforming reactions in the pre-reformer, increasing the air cooling needs of the cell and therefore reducing the temperature of the inlet air. This leads to comparable values of air utilisation factors between the two cases: 79.7% in the reference case and 75.0% for the plant with CO_2 capture. The second and most significant difference between the two configurations may be found in the reciprocal arrangement of the gas turbine H_2-rich fuel combustor and the HT air pre-heater. In the reference case, the anodic spent fuel can be burnt with the cathodic depleted air next to the cell modules (decentralised combustion); on the other hand, in the case with CCS, the use of a

Table 3
Thermodynamic conditions and chemical compositions of the main streams of atmospheric SOFC + ST power plant without CO_2 capture.

Stream	T	P	G	m	m × LHV	Composition [%mol]								
	[°C]	[bar]	[mol s^{-1}]	[kg s^{-1}]	[MW]	Ar	CH_4	CO	CO_2	C+	H_2	H_2O	N_2	O_2
1	15.0	1.00	1278.20	36.9	–	0.92	–	–	0.03	–	–	1.03	77.28	20.73
2	34.3	1.20	1278.20	36.9	–	0.92	–	–	0.03	–	–	1.03	77.28	20.73
3	672.6	1.19	1278.20	36.9	–	0.92	–	–	0.03	–	–	1.03	77.28	20.73
4	752.9	1.15	1278.20	36.9	–	0.92	–	–	0.03	–	–	1.03	77.28	20.73
5	799.9	1.12	1066.80	30.1	–	1.10	–	–	0.04	–	–	1.24	92.60	5.03
6	702.6	1.09	1066.80	30.1	–	1.10	–	–	0.04	–	–	1.24	92.60	5.03
7	1129.9	1.05	1122.60	31.2	–	1.05	–	–	1.96	–	–	7.38	88.09	1.52
8	1069.2	1.04	1122.60	31.2	–	1.00	–	–	2.00	–	–	7.40	88.10	1.50
9	817.4	1.04	1122.60	31.2	–	1.05	–	–	1.96	–	–	7.38	88.09	1.52
10	791.2	1.02	1122.60	31.2	–	1.05	–	–	1.96	–	–	7.38	88.09	1.52
11	80.0	1.01	1122.60	31.2	–	1.05	–	–	1.96	–	–	7.38	88.09	1.52
12	15.0	20.00	119.40	2.2	100.0	–	89.00	–	2.00	8.11	–	–	0.89	–
13	15.0	19.40	119.40	2.2	100.0	–	89.00	–	2.00	8.11	–	–	0.89	–
14	651.9	1.29	781.09	17.9	133.5	–	13.61	5.07	24.59	1.24	11.81	43.30	0.38	–
15	520.6	1.25	841.04	17.9	137.7	–	11.55	4.45	26.66	–	24.16	32.83	0.35	–
16	799.9	1.21	1035.30	24.7	52.5	–	–	5.99	28.67	–	13.94	51.11	0.28	–
17	799.9	1.21	661.68	15.8	33.5	–	–	5.99	28.67	–	13.94	51.11	0.28	–
18	799.9	1.21	373.59	8.9	18.9	–	–	5.99	28.67	–	13.94	51.11	0.28	–
19	716.6	1.19	373.59	8.9	18.9	–	–	6.00	28.70	–	13.90	51.10	0.30	–
20	377.1	1.18	373.59	8.9	18.9	–	–	5.99	28.67	–	13.94	51.11	0.28	–
21	340.0	1.14	373.59	8.9	18.9	–	–	5.99	28.67	–	13.94	51.11	0.28	–
22	389.3	1.12	373.59	8.9	18.2	–	–	1.01	33.65	–	18.92	46.14	0.28	–
23	352.5	1.08	373.59	8.9	18.2	–	–	1.01	33.65	–	18.92	46.14	0.28	–
24	170.6	1.06	373.59	8.9	18.2	–	–	1.01	33.65	–	18.92	46.14	0.28	–
25	82.0	1.06	373.59	8.9	18.2	–	–	1.01	33.65	–	18.92	46.14	0.28	–
26	35.0	1.03	373.59	8.9	11.1	–	–	1.01	33.65	–	18.92	46.14	0.28	–
27	35.0	1.01	212.80	6.0	18.2	–	–	1.78	59.07	–	33.22	5.44	0.50	–
28	15.0	6.31	92.33	1.1	17.9	–	–	3.86	19.61	–	75.45	–	1.08	–
29	200.0	6.31	92.33	1.1	17.9	–	–	3.86	19.61	–	75.45	–	1.08	–
30	32.2	0.048	460.72	8.3	–	–	–	–	–	–	–	100	–	–
31	32.3	6.60	300.86	5.4	–	–	–	–	–	–	–	100	–	–
32	104.1	5.60	300.86	5.4	–	–	–	–	–	–	–	100	–	–
33	130.0	6.47	458.50	2.8	–	–	–	–	–	–	–	100	–	–
34	113.1	5.60	482.37	8.3	–	–	–	–	–	–	–	100	–	–
35	139.9	3.60	482.01	8.7	–	–	–	–	–	–	–	100	–	–
36	140.6	51.02	482.01	8.7	–	–	–	–	–	–	–	100	–	–
37	207.5	50.00	482.02	8.7	–	–	–	–	–	–	–	100	–	–
38	245.4	40.00	314.55	5.7	–	–	–	–	–	–	–	100	–	–
39	250.4	40.00	314.83	5.7	–	–	–	–	–	–	–	100	–	–
40	400.0	38.60	314.55	5.7	–	–	–	–	–	–	–	100	–	–
41	245.4	40.00	167.47	3.0	–	–	–	–	–	–	–	100	–	–
42	250.4	40.00	167.62	3.0	–	–	–	–	–	–	–	100	–	–
43	400.0	38.60	167.47	3.0	–	–	–	–	–	–	–	100	–	–
44	398.0	36.67	482.02	8.7	–	–	–	–	–	–	–	–	–	–
45	32.2	0.05	460.72	8.3	–	–	–	–	–	–	–	–	–	–
46	149.2	3.79	23.87	0.4	–	–	–	–	–	–	–	–	–	–
47	108.6	1.37	37.19	0.7	–	–	–	–	–	–	–	–	–	–
48	35.0	1.01	108.90	4.7	0.31	–	–	0.20	98.81	–	0.94	–	0.06	–

centralized CO_2 purification unit favours also a centralized combustion system.

The reader shall also notice that the rationale behind the different arrangements considered in the two plants is purely technical: no variations in the overall cycle efficiency are expected as no thermodynamic values are affected. The main disadvantage of placing the high temperature air pre-heater downstream the combustor lies in the materials operating temperature of the heat exchanger, i.e. components lifetime expectations and costs. However, it is believed that some of these issues may be partly overcome by an appropriate configuration design of the heat exchanger.

It is worth noting that in this configuration there might be room for medium-to-low grade heat recovery in the CCS section. Accordingly, a CO_2 capture technology based on thermal regeneration, e.g. physic-chemical scrubbing (see also section 7), could lead to higher electrical efficiency compared to the cryogenic condensation (which requires additional compression energy). On the other hand, while the cryogenic condensation is a rather simple technology, the complexity of an absorption process together with issues on amines degradation, vapour formation and handling of toxic chemical compounds, would introduce several drawbacks. Therefore, with the aim of keeping the plant complexity limited, removal of CO_2 by cryogenic process is here preferred.

5. Comparison of the power cycles

Table 4 reports the overall performance obtainable with the proposed power plant configurations, in comparison with the corresponding cases without capture. In terms of power balances, for the given assumption of 100 MW_{LHV} entering power, the net power output exceeds 70 MW_{el} in both cases (net power, including the consumption of the intercooled compressor), of which 68 MW_{el} from the SOFC and around 7.68 MW from the steam turbine or 5.6 MW_{el} from the gas turbine. This results in a net electric efficiency of 71.49% for the SOFC + SC and 70.82% for the SOFC + GT.

It is worth noting the high ratio between the fuel cell and the

Table 4
Thermodynamic properties and chemical compositions of the plant streams for the SOFC + GT plant with CO_2 capture.

Stream	T	P	G	m	m × LHV	Composition [%mol]								
	[°C]	[bar]	[mol s^{-1}]	[kg s^{-1}]	[MW]	Ar	CH_4	CO	CO_2	C+	H_2	H_2O	N_2	O_2
1	15.0	1.01	1498.40	43.2	–	0.92	–	–	0.03	–	–	1.03	77.28	20.73
2	89.7	2.07	1498.40	43.2	–	0.92	–	–	0.03	–	–	1.03	77.28	20.73
3	35.0	2.03	1498.40	43.2	–	0.92	–	–	0.03	–	–	1.03	77.28	20.73
4	111.4	4.07	1498.40	43.2	–	0.92	–	–	0.03	–	–	1.03	77.28	20.73
5	450.0	3.94	1498.40	43.2	–	0.92	–	–	0.03	–	–	1.03	77.28	20.73
6	450.0	3.94	138.24	4.0	–	0.92	–	–	0.03	–	–	1.03	77.28	20.73
7	450.0	3.94	1360.20	39.2	–	0.92	–	–	0.03	–	–	1.03	77.28	20.73
8	559.5	3.94	1360.10	39.2	–	0.92	–	–	0.03	–	–	1.03	77.28	20.73
9	735.0	3.83	1360.10	39.2	–	0.92	–	–	0.03	–	–	1.03	77.28	20.73
10	800.0	3.71	1148.70	32.5	–	1.09	–	–	0.04	–	–	1.22	91.50	6.15
11	590.4	3.60	1148.70	32.5	–	1.09	–	–	0.04	–	–	1.22	91.50	6.15
12	575.4	3.60	1287.00	36.5	–	1.07	–	–	0.04	–	–	1.20	89.98	7.71
13	950.1	3.49	1342.70	37.5	–	1.03	–	–	1.65	–	–	6.34	86.32	4.67
14	679.2	1.04	1342.70	37.5	–	1.03	–	–	1.65	–	–	6.34	86.32	4.67
15	319.6	1.01	1342.70	37.5	–	1.03	–	–	1.65	–	–	6.34	86.32	4.67
16	15.0	20.00	119.41	2.2	100.0	–	89.00	–	2.00	8.11	–	–	0.89	–
17	15.0	19.40	119.41	2.2	100.0	–	89.00	–	2.00	8.11	–	–	0.89	–
18	200.0	19.01	119.41	2.2	100.0	–	89.00	–	2.00	8.11	–	–	0.89	–
19	677.2	3.91	781.10	17.9	133.5	–	13.61	5.07	24.59	1.24	11.81	43.30	0.38	–
20	574.9	3.80	828.65	17.9	136.8	–	12.47	4.99	25.84	–	21.06	35.29	0.36	–
21	800.0	3.68	1035.30	24.7	52.5	–	–	5.99	28.67	–	13.94	51.11	0.28	–
22	800.0	3.68	661.70	15.8	33.5	–	–	5.99	28.67	–	13.94	51.11	0.28	–
23	800.0	3.68	373.60	8.9	18.9	–	–	5.99	28.67	–	13.94	51.11	0.28	–
24	519.4	3.59	373.60	8.9	18.9	–	–	5.99	28.67	–	13.94	51.11	0.28	–
25	457.3	3.59	373.60	8.9	18.9	–	–	5.99	28.67	–	13.94	51.11	0.28	–
26	424.8	3.44	373.60	8.9	18.9	–	–	5.99	28.67	–	13.94	51.11	0.28	–
27	340.0	3.44	373.60	8.9	18.9	–	–	5.99	28.67	–	13.94	51.11	0.28	–
28	389.3	3.38	373.60	8.9	18.2	–	–	1.01	33.65	–	18.92	46.14	0.28	–
29	35.0	3.31	373.60	8.9	10.7	–	–	1.01	33.65	–	18.92	46.14	0.28	
30	35.0	3.27	204.71	5.9	18.2	–	–	1.85	61.41	–	34.53	1.70	0.52	
31	35.0	9.17	92.33	1.1	17.9	–	–	3.86	19.61	–	75.45	–	1.08	
32	200.0	8.98	92.33	1.1	17.9	–	–	3.86	19.61	–	75.45	–	1.08	
33	35.0	3.27	108.90	4.7	0.3	–	–	0.20	98.81	–	0.94	–	0.06	
34	480.0	20.41	768.02	33.8	–	–	–	–	100	–	–	–	–	
35	489.4	21.68	768.03	33.8	–	–	–	–	100	–	–	–	–	
36	600.0	20.82	768.02	33.8	–	–	–	–	100	–	–	–	–	

total power, with the FC generating about 90% of the gross power output, which makes on one hand the plant very efficient but on the other hand increases the dependency on the FC cost and technology readiness. The CO_2 separation and compression system accounts for 3.14% and 4.34% of the plants gross power output, respectively for the pressurised and atmospheric case. The reduction of the net electric efficiency in comparison to the reference cases without CO_2 capture is particularly low for the SOFC + SC case, whose efficiency decreases by only 3.7% points. In this case, the efficiency penalty is basically related to the auxiliary consumptions of the CO_2 separation and compression unit. For the SOFC + GT the efficiency penalty is more significant: about 7.9% points. In this case, significant additional penalties are due to the low temperature heat losses that are unrecoverable with a GT-based bottoming power cycle (unless adding an additional lower temperature bottoming cycle; note also that the GT cycle pressure ratio has been kept equal to the case without CCS).

In Table 5 the CO_2 emission performance of the considered power plants has also been summarised by means of absolute and differential parameters with respect to the reference cases without CCS. It is worth noting that, because of the significant fraction of incondensable gases still present in the stream entering the cryogenic unit (H_2+CO > 35%) and the resulting CO_2 separation efficiency (85.6%), the CO_2 capture ratio is about 83% for both the considered configurations because the cryogenic process inlet stream is very similar. Considering the CO_2 avoided figures, SOFC + SC reaches 82.1% while SOFC + GT 81%. The departure from the CCR, which is equal for both cases, is determined by the different decrease in the net electric efficiency compared to the case without capture. Considerations about the possibility to increase the CO_2 capture efficiency are discussed in Section 3. However, even if lower than the typical 90% capture target of CCS power plants, the 81–82% level is remarkable in light of the high efficiencies achieved.

Finally, the SPECCA parameter is used to evaluate the primary energy consumption specific to the CO_2 avoided, as indicated in Eq. (3):

$$SPECCA = \frac{3600\ \left(\frac{1}{\eta} - \frac{1}{\eta_{ref}}\right)}{E_{CO_2\,ref} - E_{CO_2}} \quad \left[\frac{MJ}{kg_{CO_2}}\right] \tag{3}$$

The SPECCA shows that the pressurised configuration consumes a larger amount of primary energy to reduce the CO_2 emissions compared to the atmospheric case. The main reason of this is again due to the different efficiency penalty obtained in the two cases assessed with respect to the corresponding cases without CO_2 capture. As mentioned in the previous sections, part of the disadvantage in terms of efficiency could be covered by installing an additional ORC bottoming cycle, recovering the significant amount of heat dissipated to the environment at medium-high temperature. In any case, the selection of the best configurations of the two proposed cannot be exempted from a detailed economic analysis [38,39] as proposed in literature for other fuel cell plant with CO_2 capture [40,41].

By the point of view of a thermodynamic analysis, a second-law

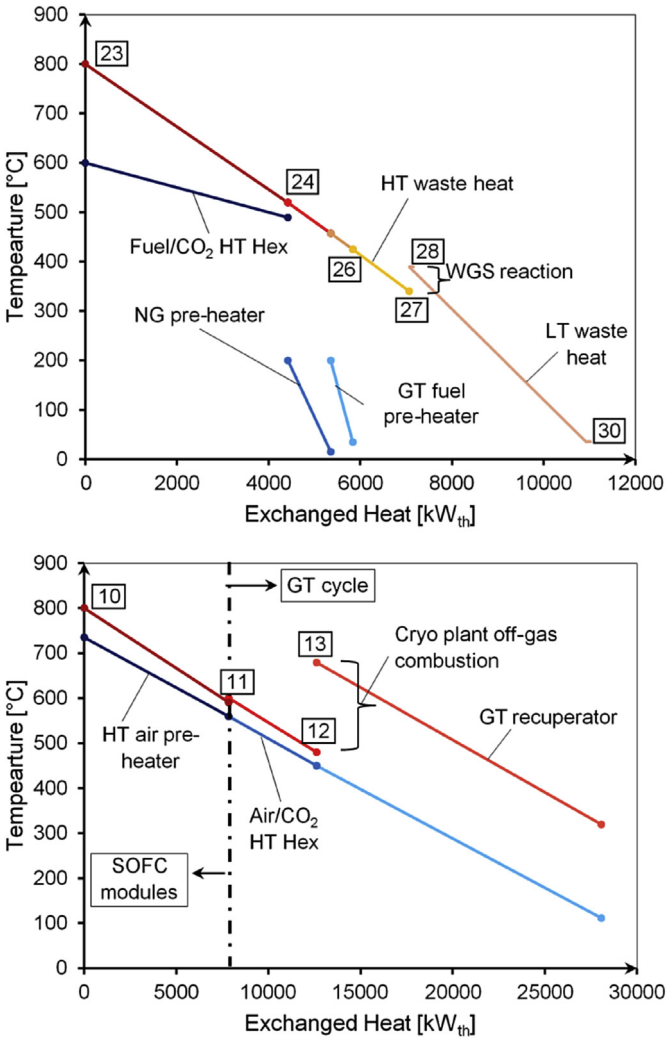

Fig. 5. Cumulative Temperature-Heat duty diagram of anodic spent fuel (stream #23 in Fig. 4) cooling section (above) and of cathode exhaust (stream #10 in Fig. 4) cooling section (below).

Table 5
Overall energy balances of pressurised (SOFC + GT) and atmospheric (SOFC + ST) power plants, with CO_2 capture section and comparison with corresponding cases without CO_2 capture.

	Atmospheric plant (SOFC + ST)		Pressurised plant (SOFC + GT)	
CO_2 capture	No	Yes	No	Yes
Fuel Inlet (LHV) [MW]	100	100	100	100
Fuel Cell net power [MW]	68.06	68.06	68.06	68.06
GT net power [MW]	–	–	10.71	5.6
ST power [MW]	8.06	7.68	–	–
aux electric power [MW]	−0.91	−4.24	−0.03	−2.83
overall net power [MW]	75.20	71.49	78.74	70.82
net electric efficiency HHV [%]	67.93	64.59	71.14	63.99
net electric efficiency LHV [%]	75.20	71.49	78.74	70.82
LHV efficiency penalty [% points]	–	−3.78	–	−7.92
Carbon capture ratio [%]	–	82.97	–	82.92
CO_2 emissions [kg s^{-1}]	5.72	0.970	5.72	0.973
E_{CO2} [kg MWh^{-1}]	273.59	48.86	260.50	49.46
CO_2 avoided [%]	–	82.14	–	81.01
SPECCA [MJ kg$^{-1}_{CO2}$]	–	1.11	–	2.42

evaluation of the two considered power plants yields the results reported in Table 6. Losses are divided according to the same repartition introduced in Part A of the work, to which the CO_2 separation losses (XIV and XV) have been added.

As a result of CO_2 capture process, the second-law efficiency decreases in both power plants compared to the equivalent configurations without CCS. It is worth noting that the efficiency reduction for the SOFC + SC case – which consists of about 3.5% of the total exergy available from the inlet fuel – is close to the additional loss related to the cryogenic process (3.1%), indicating that the addition of CCS does not alter the plant thermodynamic optimization. Nevertheless, it can be noted that the SOFC + SC configuration experiences a redistribution of the heat transfer losses compared to the corresponding case without CCS; in fact, the losses on the HT air pre-heater reduce as the majority of the thermal duty is shifted towards the LT air pre-heater, which exploits the remaining enthalpy content of the exhaust gases in order to mini-mise the stack losses. On the other hand, because of the larger low temperature waste heat and heat transfer losses which characterise the anodic spent gases cooling section, the SOFC + GT power plant configuration is affected by a larger efficiency penalty (6.6%) compared to the plant without CCS. The majority of exergy dissi-pation is concentrated in stack and waste heat losses (line XI in Table 6); as already mentioned, the addition of a bottoming cycle (e.g. ORC) –not considered here for simplicity - could exploit part of the waste heat and allow reaching a net efficiency practically equal to the SOFC + ST case, despite the higher plant complexity.

6. Sensitivity analysis

In this section the sensitivity analyses on two of the most important cell operating parameters are presented: (i) the cell voltage, and (ii) the fuel utilisation factor. The plant always work with a total fuel input of 100 MW_{th}. As far as the first parameter is concerned, the fuel cell is considered to be operated at constant global fuel utilisation factor U_f, equal to that of the case without capture (U_f = 85.0%). Consequently, a change of voltage involves one of the following implications: (i) the cell technological level changes, and so does its power output, while the current density of the cell and its active area remain constant, or (ii) for a given cell technology, the current density and the cell active area change (also here, at constant active area if the power output is constant). The first case implies a change of the fuel cell type or generation (e.g. with different materials, geometries, manufacturing processes allowing for instance increasing the voltage with the same current density and U_f), while in the second case the size of the SOFC unit is affected.

The second varied parameter is the fuel utilisation factor. This analysis is carried out considering the same cell voltage as that of the reference case (V = 0.86 V). Similarly to the previous case, this can be achieved by assuming either a variation of the cell technology (i.e. allowing to keep the same constant current density despite varied fuel species concentration) or a change of the current density according to the polarization curves of the cell technology. In both cases, an increase of the SOFC unit size is expected when U_f is increased, due to the increase of the absolute current extracted from the fuel cell system.

6.1. Voltage sensitivity analysis

6.1.1. SOFC + SC plant with CCS

At lower cell voltages with respect to the reference case, the amount of the fuel chemical energy converted into thermal energy rather than into electricity increases. This requires raising the air mass flow in order to meet the cooling needs of the cell, therefore

Table 6
Second law analysis of the considered cycles.

	Cycle configuration with CO_2 capture	
II law losses $\Delta\eta_{II}$ (%)	Atmospheric SOFC + ST	Pressurised SOFC + GT
I. SOFC Electrochemical Reactions	3.602	3.475
II. Other SOFC losses	3.344	3.403
III. Combustor	4.185	4.770
IV. Air blower/compressor	0.132	0.579
V. Turbine	–	0.557
VI. Mech., el. and auxiliary	0.044	0.212
VII. Recuperator	–	2.554
VIII. Air HT pre-heater	0.290	0.405
IX. HRSG	5.367	–
X. Other heat and pressure losses	5.037	4.168
XI. Stack/Waste heat losses	1.272	7.106
XII. Pre-reformer/WGS	0.537	0.416
XIII. Steam cycle	2.539	–
XIV. CO_2 separation section	3.099	2.205
XV. CO_2 to storage	2.267	2.559
II law efficiency η_{II}	68.285	67.591
Inlet fuel exergy [MW]	104.97	104.97

progressively reducing the air utilisation factor from 78.9% to 15.4% when voltage goes from 0.86 V to 0.72 V. Accordingly, the oxygen content at the combustor inlet increases, while the combustor outlet temperature reduces because of the larger amount of inert gases. These effects may be observed in the reduction of the specific work referred to the air flow (from 1846 kJ kg_{air}^{-1} to 318.7 kJ kg_{air}^{-1}) as the cell power output reduces with voltage. A quantitative analysis of these figures suggests that the air specific work reduces more than proportionally when the voltage reduces. On the other hand, on the anode side a proportional reduction of the specific work referred to the fuel flow occurs (from 3793 kJ kg_{fuel}^{-1} to 3176 kJ kg_{fuel}^{-1}- the fuel mass flow does not change). This behaviour shifts the cooling needs of the cell from the fuel side to the air side; this, however, does not deeply change the bottoming cycle heat exchangers operating conditions, which always respect the constraints on the minimum allowed ΔTs.

From a power balance perspective, the reduction of the cell voltage strongly affects the cell power output, which drops from 68.1 MW_{el} at the design point (V = 0.86 V) to 57 MW_{el} at V = 0.72 V. The effect on the overall net power output (see Fig. 6) is partly compensated by the higher power of the steam cycle, which is able to recover part of the thermal energy that the cell does not directly exploit. Along with the steam cycle power, the auxiliaries power increases as well. This is mainly connected to air blower consumption, which increases by a factor of 4 when the cell voltage is reduced in the investigated range. The cryogenic CO_2 separation process is practically not influenced, since the utilisation factor has been kept constant (i.e. the composition at the cell outlet does not change).

At cell voltage higher than the nominal, the SOFC module suffers a lack of available heat, complicating the thermal management of the SOFC module components. Due to that, simulations at voltage 0.88 V and 0.9 V were carried out with some modifications with respect to the other cases. Firstly, an additional heat exchanger (anodic pre-heater) is introduced in order to increase the anode inlet temperature at point #15, exploiting the available heat in the non-recycled anodic stream (point #18). Secondly, a reduction of the thermal losses assumption (1.8% at V = 0.88 V and 0.8% at V = 0.90 V) was considered, in line with the assumption of relying on more performing stacks. As a result it was possible to keep the cathode inlet temperature at 735 °C – equal to the reference value – for case at V = 088 V, while the case at V = 0.90 V requires a limited temperature increase at cathode inlet, up to 765 °C.

The addition of the anodic pre-heater shifts back to the air flow

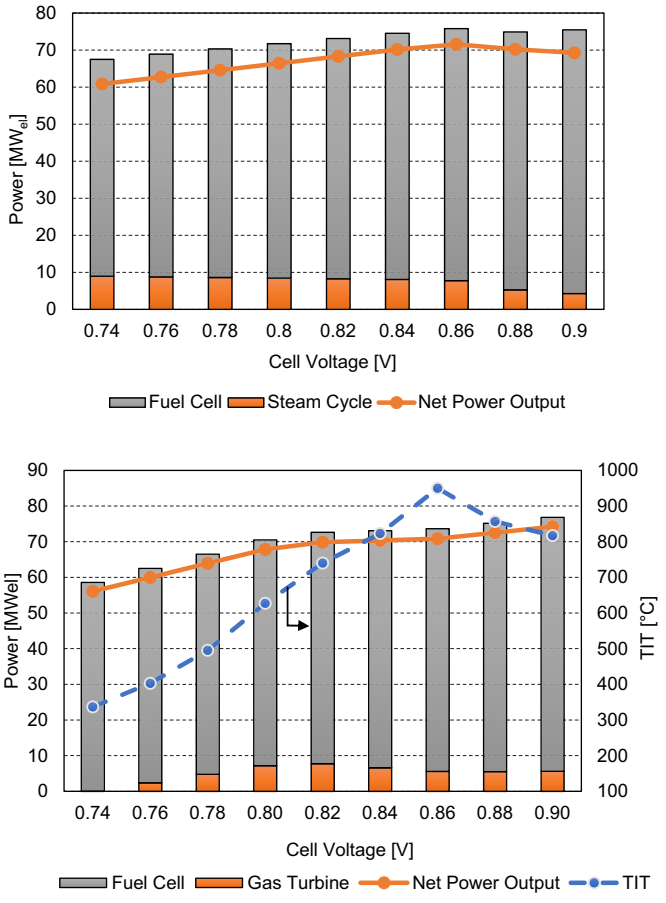

Fig. 6. Sensitivity analyses on cell voltage for the SOFC + SC plant with CCS (above) and SOFC + GT plant with CCS (below).

part of the cooling load of the cell, thus entailing a rise of the air mass flow rate (reduction of the air specific work), required to: i) meet the minimum temperature difference constraints on the air pre-heater; ii) meet the minimum O_2 constraint on the cathode and combustor outlet flows. On one hand, this determines an increase of plant stack losses due to the higher air excess flow rate and flue gas heat loss to environment; on the other hand, the anodic pre-

heating reduces the thermal power input to the steam cycle, thus its power output, resulting in an overall loss of power production and efficiency (despite the SOFC power output rise).

6.1.2. SOFC + GT plant with CCS

Similarly to the previous case, a reduction in the cell voltage is conducive to an increase of the air flow rate. The main consequence of this change is the reduction of the turbine inlet temperature which determines an overall reduction of the gas turbine power output. As shown in the lower part of Fig. 6, a maximum TIT is obtained in the analysis for V = 0.86. At low voltage this is a consequence of the increasing air flow rate to cool the SOFC and of the constant availability of GT fuel (off gas from the CO_2 separation unit), leading to an increased air-to-fuel ratio, therefore to a lower combustion temperature. At high voltage, the air flow rate cannot be reduced further at the given fuel utilisation factor, because it is limited by the oxygen availability determined by the minimum O_2 concentration at SOFC outlet. Therefore, air ΔT in the fuel cell reduces as losses decrease (i.e. voltage increases). Accordingly, the air (stream #9) inlet temperature has to be increased by cooling the cathode off-gas (stream #11) to lower temperature in the HT air preheater. The effect of the lower temperature of the oxidant in the GT combustor reflects again in a lower TIT.

It is also noteworthy that, when the voltage approaches 0.74 V, the turbine outlet temperature approaches the GT compressor outlet temperature, making the amount of heat recovered in the recuperative heat exchanger negligible. It is also observed that the gas expander power output is overcome by the air compression power below 0.74 V, calling for an electric motor to drive the air compressor instead of an electric generator. Interestingly, Fig. 6 shows that the gas turbine engine experiences a maximum in its power generation when the cell voltage equals 0.82 V. This behaviour is related to the opposing effect of a variation in the turbine mass flow rate and in the TIT. A global maximum exists because at higher cell voltages the lower mass flow rate compensates the effect of the higher TIT on the GT specific work, whilst at lower cell voltages the opposite trend occurs.

The same layout modification strategies chosen in the atmospheric case to adjust the thermal balances can been adopted herein for the cases at higher voltage: the anode inlet stream is preheated up to 630 °C at V = 0.88 V and to 645 °C at V = 0.90 V, exploiting the non-recycled anodic off-gas thermal content. Conversely to the SOFC + SC plant, the overall plant performance rises due to the fact that the GT power output is not strongly affected by such plant configuration change.

In conclusion, the pressurised SOFC + GT configuration features a higher sensitivity to the fuel cell voltage variation compared to the SOFC + SC case, with a progressive increase of overall efficiency at higher voltage and a steeper decrease at lower voltages. The main explanation lays in the superior capability of the steam cycle to exploit low temperature waste heat, which is increasingly important at low voltages (in other terms, as already pointed out, the SOFC + GT would need the addition of a Rankine bottoming cycle to overcome this limitation).

6.2. Fuel utilisation factor sensitivity

Differently from the sensitivity analysis on the cell voltage, a change in the fuel utilisation factor U_f entails a variation in the composition of cell outlet. This requires the evaluation of the CCS performance for every U_f considered. In particular, when U_f increases, the SOFC generates a lower concentration of un-oxidised species at the cell outlet and a higher quantity of CO_2 at the cryogenic process inlet stream, which thus guarantees a higher capture ratio. Cell voltage has been maintained at the reference value of 0.86 V. Therefore, when U_f is increased, an increase of the SOFC active area has to be expected because of (i) the reduction of current density necessary to achieve the same voltage with lower average concentration of fuel species, and (ii) the increase of the current needed to transfer an increased amount of oxygen trough the electrolyte. From the energy balance point of view, with the increase of U_f and the consequent larger amount of oxidised fuel, the cell increases the thermal energy generated which in turn requires a higher air mass flow for cooling. The resulting performance is strictly dependent on the bottoming cycle configuration.

In this work, fuel utilisation factors up to 92% have been considered, allowing to reach CO_2 capture rates in excess of 90%. Notably, recent stack tests reported in Ref. [42], have explored the performance of anode-supported cells operated under high fuel utilisation factors (up to U_f = 90%); however, these working conditions require careful consideration due to the presence of a trade-off between their beneficial effects on the thermodynamic and environmental performance of the plant and the jeopardised lifetime expectations of the stacks.

6.2.1. SOFC + SC plant with CCS

Results of the U_F sensitivity analysis are shown in Fig. 7. As expected, the rise of cell power output at higher U_f overcompensates the decrease of the steam cycle power output; accordingly, the plant efficiency increases at higher U_f.

Similarly to the nominal operating point, where the global U_f is 85.0%, also the cases with U_f = 85.8% and U_f = 84.1% are influenced by the assumed O_2 molar fraction constraint at the cathode outlet.

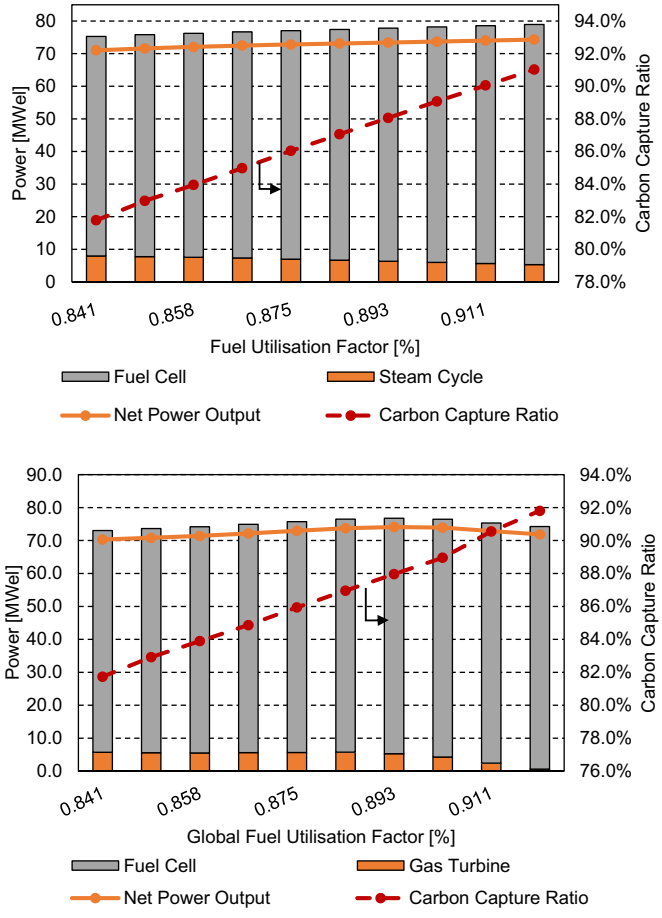

Fig. 7. Sensitivity analyses on cell fuel utilisation factor for the SOFC + SC plant with CCS (above) and for the SOFC + GT plant with CCS (below).

In order to cope with this assumption, the air inlet temperature has been increased to 745 °C and 765 °C, respectively for the two cases, thus raising the cooling needs of the cell and the required air mass flow rate at the cathode inlet. Following the change in the anode exhaust composition, the cryogenic process features a different capture efficiency (reported on the secondary axis of Fig. 7). As expected, a higher fuel utilisation factor is conducive to a larger CO_2 molar fraction at the cell outlet and therefore to higher capture efficiency (up to 91%), if the operating parameters of the CO_2 separation unit are kept constant.

Furthermore, an analysis on the primary energy consumption required to increase the CCR at higher U_f values shows a reduction of the SPECCA figure compared to cases operating at lower U_f. In particular, it is noted that the SPECCA is characterised by a monotonically decreasing profile from the lowest $U_f = 0.841$ to the highest one ($U_f = 0.92$), respectively from 1.105 MJ kg_{CO2}^{-1} to 0.873 MJ kg_{CO2}^{-1}. Each SPECCA value has been evaluated with refer-ence to a power plant equal to the SOFC + SC without CCS explained in Part A, where the cell was operated at the corresponding U_f. The positive effect of increasing U_f on the SPECCA is almost solely related to the increase of CO_2 capture rate and hence to the reduction of the specific emissions, while minor effects are observed on the efficiency difference between cases with the same fuel utilisation.

6.2.2. SOFC + GT plant with CCS

Fig. 7 shows also the results of the U_F sensitivity analysis in term of fuel cell power and gas turbine power for the SOFC + GT plant with CCS (lower part of the figure). Compared to the atmospheric case, this plant generally requires a more careful management of the components when the operating parameters of the cell are varied.

It can be noted that at increasing U_f, two counteracting effects take place: (i) the oxidant mass flow rate rises in order to respect the thermal balance of the cell, with a potential benefit on the GT output, while (ii) the temperature at the air preheater exit (point #11 in Fig. 5) decreases (although always respecting the assumptions of $\Delta T_{min} = 30$ °C) to keep the cathode inlet temperature constant. The latter effect contributes to decreasing the gas turbine TIT, along with the lower residual heating value of the anode off-gas reaching the GT combustor (point #32). Conversely to the atmospheric case, due to the progressive increase of air mass flow rate, the operating condition is not characterised by any issues related to the minimum O_2 molar fraction at the cell outlet.

As far as the overall plant efficiency is concerned, the presence of a global maximum shall be highlighted at $U_f = 90.2\%$; this maximum coincides with the best trade-off between the reduction of gas turbine and the rise of the SOFC power output at the highest utilisation factors. This consideration leads also to the explanation of the presence of a minimum in the SPECCA parameter at

$U_f = 90.2\%$ equal to 1.53 MJ kg_{CO2}^{-1}. On the other hand, the maximum SPECCA is reached at the lowest $U_f = 84.1\%$, equal to 2.50 MJ kg_{CO2}^{-1}, whilst the highest U_f is characterised by SPECCA = 1.79 MJ kg_{CO2}^{-1}.

An additional minor modification required by the plant is related to the maximum operating pressure of the cryogenic process, which has to be increased at the highest utilisation factors (respectively imposing 45 bar and 43 bar at $U_f = 92.0\%$ and $U_f = 91.1\%$ respectively) in order to avoid the risk of dry ice formation.

As highlighted for the sensitivity analysis on the cell voltage, the atmospheric plant features a higher performance stability compared to the pressurised case; this applies also when the cell works at different utilisation factors compared to the reference case.

6.3. Air utilisation factor sensitivity

As it has been pointed out in the part A of this study, all simulations adopt a high U_a, which is limited in order to have a 5% minimum O_2 molar fraction at the cathode outlet. This specific operating condition may require dedicated flow field configurations and distribution patterns in order for the cell voltage to comply with the lower local Nernst potential induced by the intense reactant consumption, as discussed in literature for the case of coal based cycles [43]. Therefore a sensitivity analysis on the air utilisation factor has been carried out in order to evaluate its effects on the overall plant performance.

Fig. 8 reports the results of the sensitivity analysis on the SOFC + SC and SOFC + GT with CCS focusing on lower (thus less demanding) values of U_a compared to the reference cases (which are 79.8% and 75.0% respectively).

6.3.1. SOFC + SC plant with CCS

As far as the SOFC + SC plant is concerned, the operation of the cell at the outlet temperature of the reference case (800 °C), implies that the independent parameter used to adjust U_a is the cathode inlet temperature. Indeed, this variable affects the amount of air mass flow rate required to meet the cooling needs of the cell. As a result, when U_a is reduced from about 80% to approximately 50%, the cathode inlet temperature increases from 753 °C to 770 °C.

As it has already been highlighted in the voltage and U_f sensitivity analyses, it is worth evaluating the new SOFC operating conditions by means of the difference in specific work of the cell; in particular, the air specific work is reduced from 1846.2 kJ kg^{-1} to 1181.6 kJ kg^{-1} going from $U_a = 80\%$ to $U_a = 50\%$ due to the rise of the air mass flow rate; this similarly reproduces the operating condi-tions at high U_f. On the other hand, the fuel specific work remains constant at 3793.3 kJ kg^{-1}.

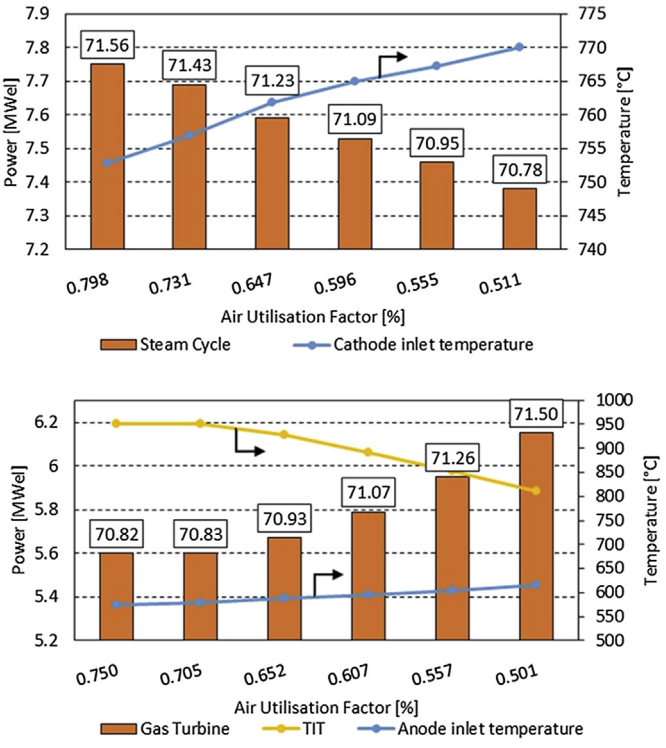

Fig. 8. Sensitivity analyses on cell air utilisation factor for the SOFC + SC plant with CCS (above) and for the SOFC + GT plant with CCS (below). The data labels show the overall net power plant efficiency LHV.

The main consequence of the rise in the air mass flow rate is the reduction of the combustor outlet temperature and an increase of the stack losses due to the larger flue gas flow rate. This entails a drop of the steam cycle power output of nearly 4.7% compared to the reference case with CCS. However the contribute of the steam cycle to the total power output is relatively limited, and the overall cycle efficiency only decreases by approximately 1% when Ua is decreased from 80% to 50%. Accordingly, more conservative hy-pothesis on the air utilisation factor would not lead to a significant performance decrease a.

2.3.2 SOFC + GT plant with CCS.

The result of the sensitivity analysis on U_a for the SOFC + GT case shows a more interesting behaviour compared to the atmospheric case. First, as shown in Fig. 8, the independent parameter used to adjust U_a is the anode inlet temperature and not the cathode inlet temperature as in the SOFC + SC case. The change in the independent parameter was required to comply with the minimum temperature difference requirement (30 °C) on the high temperature air pre-heater. By means of an anodic stream pre-heater (as it has been employed in the sensitivity analysis vs. high voltages) the anode inlet temperature has been increased, from 575 °C at $U_a =$ 75.0% to 615 °C at $U_a = 50.0\%$, exploiting the available thermal power of the non-recycled stream. Higher anode inlet temperature calls for larger cooling need in the cell and, therefore, larger cathodic air mass flow rate.

The rise of the air mass flow rate leads to a reduction in the bypass air (stream #6), which is required to comply with the maximum TIT of the gas turbine engine. Additionally, below $U_a =$ 70%, this stream becomes unnecessary since the TIT is always below 950 °C and progressively reduces down to ~810 °C. The analysis is carried out for simplicity keeping constant the pressure ratio ($\beta = 4$). As per the atmospheric case, the air specific work of the SOFC reduces (from 1734.4 kJ kg^{-1} at $U_a = 75\%$ to 1160.4 kJ kg^{-1} at $U_a =$ 50.0%) whilst the fuel specific work remains constant (3793.3 kJ kg^{-1}).

Interestingly, as the air utilisation factor is reduced, the overall plant performance slightly increases despite the lower TIT. The main reason is related to the better performance of the low tem-perature regenerative pre-heater of the gas turbine cycle, which works with lower average temperature differences and higher effectiveness. This results from the lower turbine outlet tempera-ture (#14 in Fig. 4) and the lower stack temperature (#15, decreasing from 319 °C to 206 °C), entailing a reduction of the exhaust waste heat despite the increased gas flow rate. Conse-quently, the cycle experiences an overall beneficial effect, with a net efficiency gain of approximately 0.7%, primarily given by a larger gas turbine power output (0.6 MW) and a slight reduction of auxiliary consumptions (blower of the high temperature CO_2 loop).

7. Options for increasing the CO_2 capture efficiency

It is noteworthy that the power plants proposed so far are characterised by a carbon capture efficiency which may not be always comparable to those of more conventional carbon capture technologies [3,4]. In fact, if the cases at the reference fuel utilisation factors are considered, the resulting CCR are about 83% in both the atmospheric and pressurised configurations. The relatively low CO_2 capture efficiency is due to the relatively low CO_2 concentration (about 60% on dry basis) in the stream entering the cryogenic unit. If higher figures were required (i.e. CCR >90%), new solutions might be proposed, other than following the path of increasing the operating value of U_f (as already shown in Figs. 6 and 7). In this section different solutions to this issue are introduced. They all eventually entail a slight decrease of the plant electric efficiency. The reader can make reference to future work on this subjects for the details of these simulations.

The first solution proposed hereby is the employment of methods for recovering part of the CO_2 lost with the H_2-rich gas released from the CO_2 separation unit. Strategies of this type, based on commercial technologies, are widely assessed to increase the capture efficiency of the gas processing unit of power plants based on oxyfuel boilers and are based on using polymeric CO_2 membranes [44] or vacuum pressure swing adsorption (VPSA) systems [45]. In this work, this suggestion is based on the consideration that the H_2-rich gas contains all the CO_2 vented to the atmosphere and has a relatively high CO_2 concentration (approximately 19.6% CO_2 on a molar dry basis) in both the atmospheric and pressurised SOFC plant. With reference to the integration of a polymeric CO_2 membrane, the separation process would exploit the high pressure of the H_2-rich fuel at the regenerator HE1 outlet of Fig. 1 (40 bar) as driving force. Assuming even a modest separation efficiency of 75%, the CCR could be increased up to more than 95%, keeping a relatively high minimum CO_2 partial pressure of about 1.7 bar.

It should be noted that the adoption of such a modification in the plants configurations does also have consequences on the thermodynamic performance of the cycle; in particular, the following changes should be considered: (i) rise of the processed mass flow in the cryogenic separation unit, with consequent increment of the compression power consumption; (ii) reduction of the mass flow in the gas turbine – for the pressurised plant – and in the heat recovery section – for the atmospheric one; (iii) need of an additional compressor/vacuum pump for the recovered CO_2 stream at the membrane outlet. Therefore, a comprehensive analysis of the process integration and sensitivity analysis on the process param-eters will be needed to determine the plant performance and optimise the process.

A polymeric H_2 membrane may be also considered. This could be for example integrated after the first CO_2 compression train to recover H_2 from the pressurised gas before the cold box. Considering a compression to 40 bar and an inlet H_2 concentration of about 35%, a modest H_2 separation efficiency of 75% would allow keeping a relatively high minimum H_2 partial pressure on the membrane feed side of about 4 bar and increasing the CO_2 concentration to above 85%, boosting significantly the CO_2 recovery efficiency in the cryogenic separation process.

Other solutions to raise the CCR of the two considered plants may involve adopting other fuel oxidation processes, such as an oxy-fuel combustion system, or integrating more complex technologies such as oxide looping systems (e.g. Ca looping) [4,5]. In the firstcase, the oxidation completion of the anodic off-gases could be carried out in an oxy-fuel combustor fed with an O_2-rich stream produced in an Air Separation Unit (ASU). This configuration allows a complete capture of all the carbon atoms introduced in the cycle by the fuel and increase significantly the CO_2 concentration at the inlet of the compression and purification unit. The most evident drawback of the oxy-fuel solutions is the need of an ASU, which represents a source of non-negligible additional electric consumption and capital cost.

Eventually, a further option would be using a chemical/physical solvent separation process. High capture efficiencies could be obtained also in this case, and especially in the SOFC + GT plant some heat for solvent regeneration would be available with no efficiency penalty simply recovering part of the heat lost to the ambient. On the other hand, an additional chemical process is necessary in this case with drawbacks related to energy consumptions, capital cost, solvent management and control of additional emissions to air.

8. Conclusions

This work presented the thermodynamic analysis of two ultra-

high efficiency SOFC power cycles designed for electricity generation with CO_2 capture using natural gas as a fuel. Following the Part A work, where the cases without CO_2 capture were introduced along with the description of the simulation framework and the assumptions adopted, this Part B described and analysed in detail the plant with CO_2 capture. The fuel cell follows the specifications of a state-of-the-art advanced unit, representative of 60% + electrical efficiency SOFCs. The proposed plants are based on an integrated-reforming concept where fuel is reformed within the SOFC, operated at intermediate (about 750 °C) temperature. The CO_2 capture process considered in this work is a post-SOFC, internally refrigerated, cryogenic separation. While CO_2 is separated and sent to storage, incondensable gases (mainly H_2 and CO) are used in a combustor. Concerning the two plant configurations, the first considers a FC working at atmospheric pressure whereas the second is based on a moderately pressurised stack (named SOFC + SC and SOFC + GT, respectively). Accordingly, excess heat in the cell exhaust is recovered with a Rankine cycle in the former and with a Brayton cycle in the latter.

The two proposed plants were analysed from both first and second-law perspective. Additionally, sensitivity analyses on cell voltage and fuel utilisation factor were carried out. The achieved net electric efficiency is remarkable: 71.56% for the SOFC + SC and 70.82% for the SOFC + GT, where the latter could further improve its performance through the addition of an ORC bottiming cycle. Given that the cryogenic separation is limited by the phase equilibrium close to the CO_2 triple point, the CO_2 avoided is limited to 82.4% for SOFC + SC and 81.4% for SOFC + GT. These values are slightly lower than those typical of conventional post-combustion or pre-combustion capture solutions but are very remarkable in light of the achieved plant efficiency. Moreover, a sensitivity analysis shows the possibility of reaching 90% + capture rates when increasing the fuel utilisation up to 92%. Alternative strategies to increase the carbon capture rates are also addressed.

The SPECCA shows that the pressurised configuration requires a larger amount of primary energy to reduce the CO_2 emissions compared to the atmospheric case. The main reason of this can be found in the better capabilities of the bottoming steam power cycles in recovering the waste heat. On the other hand, the plant footprint along with the operability and flexibility may call for a simpler configuration as in SOFC + GT. Accordingly, the decision on which of the two configurations is more suitable for CO_2 capture cannot be exempted from a detailed economic analysis. Concerning the sensitivity analysis, the pressurised SOFC + GT configuration features a higher sensitivity towards a variation in the fuel cell voltage and fuel utilisation factor.

Acknowledgements

The authors wish to thank Edison SpA for partly supporting the work related to this study within Politecnico di Milano PhD program.

References

[1] IPCC, Climate Change 2013: the Physical Science Basis, Cambridge University Press, 2014.
[2] M.R.M. Abu-Zahra, L.H.J. Schneiders, J.P.M. Niederer, P.H.M. Feron, G.F. Versteeg, CO_2 capture from power plants. Part I. A parametric study of the technical performance based on monoethanolamine, Int. J. Greenh. Gas Control 1 (2007) 37–46.
[3] A.N.M. Peeters, A.P.C. Faaij, W.C. Turkenburg, Techno-economic analysis of natural gas combined cycles with post-combustion CO_2 absorption, including a detailed evaluation of the development potential, Int. J. Greenh. Gas Control 1 (2007) 396–417.
[4] N. MacDowell, N. Florin, A. Buchard, J. Hallett, A. Galindo, G. Jackson, C.S. Adjiman, C.K. Williams, N. Shah, P. Fennell, An overview of CO2 capture technologies, Energy Environ. Sci. 3 (11) (2010) 1645–1669.
[5] I. Martínez, M.C. Romano, J.R. Fernández, P. Chiesa, R. Murillo, J.C. Abanades, Process design of a hydrogen production plant from natural gas with CO_2 capture based on a novel Ca/Cu chemical loop, Appl. Energy 114 (2014) 192–208.
[6] G. Manzolini, E. Macchi, M. Binotti, M. Gazzani, Integration of SEWGS for carbon capture in natural gas combined cycle. Part B: reference case comparison, Int. J. Greenh. Gas Control 5 (2011) 214–225.
[7] D. Rastler, Program on Technology Innovation: Systems Assessment of Direct Carbon Fuel Cells Technology, Electric Power Research Institute (EPRI), 2008. Report No. 1016170.
[8] S. Campanari, M. Gazzani, M.C. Romano, Analysis of direct carbon fuel cell (DCFC) based coal fired power cycles with CO2 capture, J. Eng. Gas Turbines Power 135 (1) (2013), http://dx.doi.org/10.1115/1.4007354.
[9] V. Spallina, M.C. Romano, S. Campanari, G. Lozza, A SOFC-based integrated gasification fuel cell cycle with CO2 capture, J. Eng. For Gas Turbines Power 133 (7) (2011) 071706.
[10] T.A. Adams, J. Nease, D.P. Tucker, Energy conversion with solid oxide fuel cell systems: a review of concepts and outlooks for the short- and long-term, Ind. Eng. Chem. Res. 52 (2013) 3089–3111.
[11] T.A. Adams, P.I. Barton, High-efficiency power production from natural gas with carbon capture, J. Power Sources 195 (2010) 1971–1983.
[12] S. Campanari, Carbon dioxide separation from high temperature fuel cell power plants, J. Power Sources 112 (2002) 273–289.
[13] L. Duan, Y. Yang, B. He, G. Xu, Study on a novel solid oxide fuel cell/gas turbine hybrid cycle system with CO2 capture, Int. J. Energy Res. 36 (2012) 139–152.
[14] B.F. Moller, J. Arriagada, M. Assadi, I. Potts, Optimisation of an SOFC/GT system with CO2-capture, J. Power Sources 31 (2004) 320–326.
[15] S.K. Park, T.S. Kim, J.L. Sohn, Y.D. Lee, An integrated power generation system combining solid oxide fuel cell and oxy-fuel combustion for high performance and CO2 capture, Appl. Energy 88 (2011) 1187–1196.
[16] M. Powell, K. Meinhardt, V. Sprenkle, L. Chick, G. McVay, Demonstration of a highly efficient solid oxide fuel cell power system using adiabatic steam reforming and anode gas recirculation, J. Power Sources 205 (2012) 377–384, http://dx.doi.org/10.1016/j.jpowsour.2012.01.098.
[17] K. Foger, T. Rowe, Ultra-high-efficiency residential power system, in: 3rd European Fuel Cell Technology Applications Conference, Rome, Dec, 2009.
[18] H. Ghezel-Ayagh, Advances in SOFC development at fuelcell energy, in: 14th Annual SECA Workshop Pittsburgh, PA July 23-24, 2013.
[19] L. Mastropasqua, S. Campanari, P. Iora, M.C. Romano, Simulation of intermediate-temperature SOFC for 60%+ efficiency distributed generation, in: Proc. of ASME 2015 Power and Energy Conversion Conference, Power-Energy 2015–49373, USA, 2015.
[20] S. Campanari, M. Gazzani, High efficiency SOFC power cycles with indirect natural gas reforming and CO_2 capture, J. Fuel Cell Sci. Technol. 12 (2) (2015), http://dx.doi.org/10.1115/1.4029425.
[21] GS (Gas-steam cycles). http://www.gecos.polimi.it/software/gs.php, 2015.
[22] S. Consonni, G. Lozza, E. Macchi, P. Chiesa, P. Bombarda, Gas-turbine-based advanced cycles for power generation part A: calculation model, in: International Gas Turbine Conference, Yokohama, III, 1991, pp. 201–210.
[23] S. Campanari, P. Iora, E. Macchi, P. Silva, Thermodynamic analysis of integrated MCFC/gas turbine cycles for multi-MW scale power generation, J. Fuel Cell Sci. Tech. 4 (2007) 308–316.
[24] Aspen Plus Version 2006.5, Aspen Tech. Inc., Cambridge, USA, 2006.
[25] F. Franco, R. Anantharaman, O. Bolland, N. Booth, E. Dorst, C. Van Ekstrom, Common framework and test cases for transparent and comparable techno-economic evaluations of CO_2 capture technologies – the work of the European benchmarking task force, Energy Procedia (2010) 1–8.
[26] S. Campanari, P. Chiesa, G. Manzolini, CO_2 capture from combined cycles integrated with molten carbonate fuel cells, Int. J. Greenh. Gas Control 4 (2009) 441–451.
[27] P. Chiesa, S. Campanari, G. Manzolini, CO_2 cryogenic separation from combined cycles integrated with Molten Carbonate Fuel Cells, Int. J. Hydrogen Energy 36 (16) (2011) 10355–10365.
[28] M. Gazzani, D.M. Turi, G. Manzolini, Techno-economic assessment of hydrogen selective membranes for CO2 capture in integrated gasification combined cycle, Int. J. Greenh. Gas. Control 20 (2014) 293–309.
[29] V. White, R. Allam, E. Miller, Purification of oxyfuel-derived CO_2 for sequestration or EOR, in: Proceedings of 8th GHGT, Norway, 2006, pp. 19–22.
[30] D. Peng, D.B. Robinson, A new two-constant equation of state, Ind. Eng. Chem. Fundam. 15 (1976) 59–64.
[31] M.L. Ferrari, M. Pascenti, A.F. Massardo, Ejector model for high temperature fuel cell hybrid systems: experimental validation at steady-state and dynamic conditions, J. Fuel Cell Sci. Technol. 5 (2008) 041005.
[32] S. Consonni, F. Viganò, Waste gasification vs. conventional Waste-to-Energy: a comparative evaluation of two commercial technologies, Waste Manag. 32 (4) (2012) 653–666.
[33] G. Lozza, Bottoming steam cycles for combined gas steam power plants: a theoretical estimation of steam turbine performance and cycle analysis, in: Proc. 1990 ASME Cogen Turbo, New Orleans, LA, USA, ASME, New York, 1990, pp. 83–92.
[34] M. Carlson, T. Conboy, D. Fleming, J Pasch. “Scaling considerations for supercritical carbon dioxide (SCO2) cycle heat exchangers”, ASME Turbo Expo 2014, Dusseldorf, Germany, June 16-20, 2014.
[35] B. Marcenaro, A. Torazza, MCFC development at Ansaldo, in: Proceedings of the Fuel Cell Forum, Lucerne, Switzerland, 2006.

[36] P. Iora, S. Campanari, A. Salogni, Off design analysis of a hybrid plant with MCFC and gas turbine, ASME J. Fuel Cell Sci. Technol. 7 (3) (June 2010), http://dx.doi.org/10.1115/1.4000679.
[37] S. Quoilin, M.V.D. Broek, S. Declaye, P. Dewallef, V. Lemort, Techno-economic survey of organic rankine cycle (ORC) systems, Renew. Sustain. Energy Rev. 22 (2013) 168–186, http://dx.doi.org/10.1016/j.rser.2013.01.028.
[38] B.D. James, A.B. Spisak, W.G. Colella, Manufacturing cost analysis of stationary fuel cell systems, in: Strategic Analysis Inc. For NREL, 2012.
[39] J. Otomo, J. Oishi, T. Mitsumori, H. Iwasaki, K. Yamada, Evaluation of Cost Reduction Potential for 1 KW Class SOFC Stack Production: Implications for SOFC Technology Scenario, Dep. of Environment Systems, University of Tokyo, 2013.
[40] T. Kuramochi, W. Turkenburg, A. Faaij, Competitiveness of CO_2 capture from an industrial solid oxide fuel cell combined heat and power system in the early stage of market introduction, Fuel 90 (2011) 958–973.
[41] S. Campanari, P. Chiesa, G. Manzolini, S. Bedogni, Economic analysis of CO_2 capture from natural gas combined cycles using molten carbonate fuel cells, Appl. Energy 130 (2014) 562–573, http://dx.doi.org/10.1016/j.apenergy.2014.04.011.
[42] Q. Fang, L. Blum, R. Peters, M. Peksen, P. Batfalsky, D. Stolten, SOFC stack performance under high fuel utilization, Int. J. Hydrogen Energy 40 (2015) 1128–1136.
[43] M. Li, J. Brouwer, A.D. Rao, G.S. Samuelsen, Application of a detailed dimensional solid oxide fuel cell model in integrated gasification fuel cell system design and analysis, J. Power Sources 196 (2011) 5903–5912, http://dx.doi.org/10.1016/j.jpowsour.2011.02.080.
[44] V. White, A. Wright, S. Tappe, J. Yan, The air products—Vattenfall oxyfuel CO2compression and purification pilot plant at Schwarze Pumpe, Energy Procedia 37 (2013) 1490–1499.
[45] M. Shah, N. Degenstein, M. Zanfir, R. Kumar, J. Bugayong, K. Burgers, Nearzero emissions oxy-combustion CO2 purification technology, Energy Procedia 4 (2011) 988–995.